

Multiparameter inverse scattering: preliminary results

Glen R. Young*, Kris Innanen and Laurence R. Lines

gyoung@ucalgary.ca

Abstract

Inverse scattering is a key theoretical and practical tool in seismic imaging and inversion. With specific computational approaches it is possible to ascertain the material properties of the subsurface using scattered acoustic waves. We seek to determine multiple rock parameters such as density and bulk modulus from reflected seismic signals. In this poster we will examine results from inverse scattering in an acoustic medium with a constant 2D background and the results of inverting synthetically generated data for the 1D, 1.5D and 2D cases. This is the second half of an investigation detailed in Young et al, 2011.

Synthetic Examples

For these experiments we have fixed the model parameters at a x line length of 2500m and a depth of 1000m, we then choose a source/receiver spacing of 5m and a sampling time of 4ms. For the forward differencing calculations the time step is 0.5ms between frames and a computation grid of 10m in the x direction and 5m in the z direction.

A bandlimited Ricker wavelet at 20Hz and 128 samples long is convolved with the forward modeled data. In each case the initial velocity map was used as input into the CREWES forward differencing routines displayed, followed by a snapshot at each of 250 shotpoints comprising the gather of the receivers for that shotpoint.

Deconvolution and F-K migration is done on all direct wave subtracted shot profiles and a sample image is displayed for shotpoint 251. Subsequently a least squares inversion algorithm is applied to solve for the perturbations K and ρ from background values of the medium.

Conclusion

We are able to image the subsurface structure (scattering potential) to a good degree of accuracy. Since this is a linear Born approximation to first order only the primary(single) scattering signal is measured. Our simulations have not taken into account real world effects such as multiples(higher order terms) and anisotropic and anelastic media which are variable background effects.

In the single reflector case the data returned a good approximation to the magnitude of the velocity change in the medium. In the 4 layer case successively stronger perturbations from the background is clearly seen at each interface.

The much more complicated 2D cases also clearly display the perturbing structure. With a larger number of offsets included in the data we are able to distinguish differences in the relative contributions of the perturbation in bulk modulus and density. It must be noted that artefacts not related to the inversion process can complicate the image quality as discussed in the paper accompanying this poster.

References

Clayton, A.W. and Stolt, R.H, 1981, A Born-WKB inversion method for acoustic reflection data, Geophysics, 46, 1559-1567.

Young, G.R., Kris Innanen and Laurence R Lines, 2011, Multiparameter inverse scattering: computational approaches, CREWES Research Report 2011, 23

Acknowledgements

This investigation started out as a summer student project, funded through grants to Prof. Kris Innanen. I wish to thank him for the advice and guidance as well as the initial code as a template to develop this simulation.

Single interface model

This physically simple model demonstrates the power and accuracy of the inversion routine. Figure 1 is the velocity model used, figure 2 is the result of the migration of the forward modelled seismic data. Figures 3a, 3b display the inversion, the relative perturbation in bulk modulus and density occurs were expected. Note the slight amplitude difference between the two images. Figure 4 displays the velocity perturbation image generated from figs. 3a, 3b. The magnitude of the velocity change is the expected 1500 m/s.

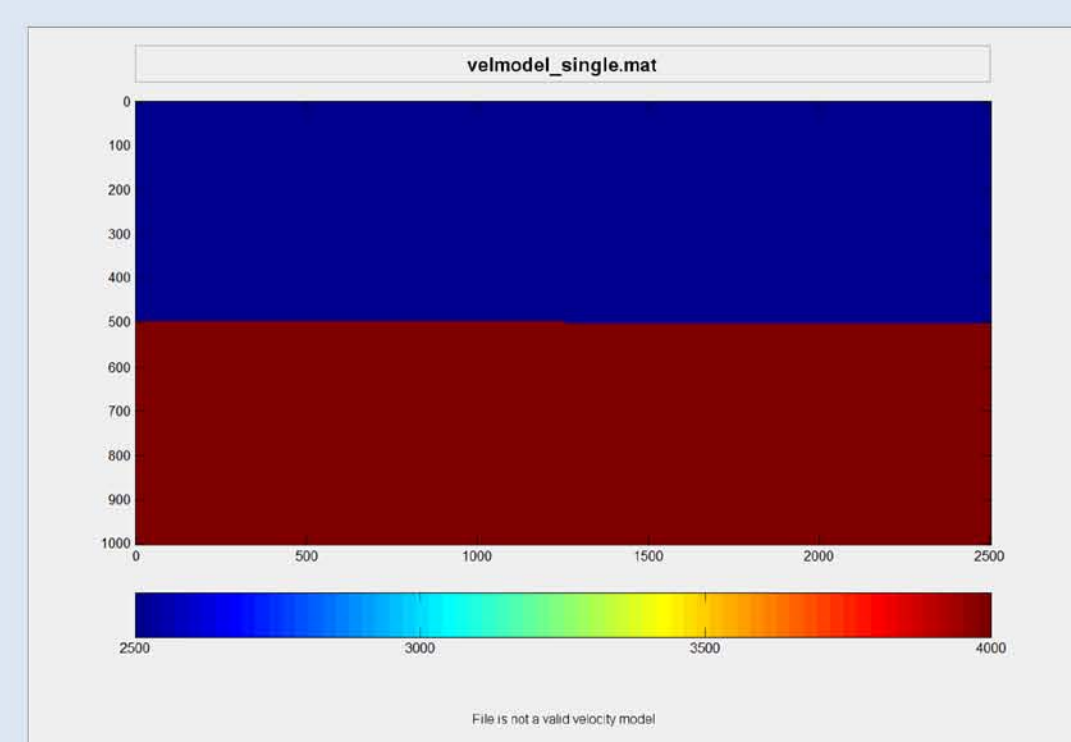


Figure 1: Two Layer Horizontal Velocity Model

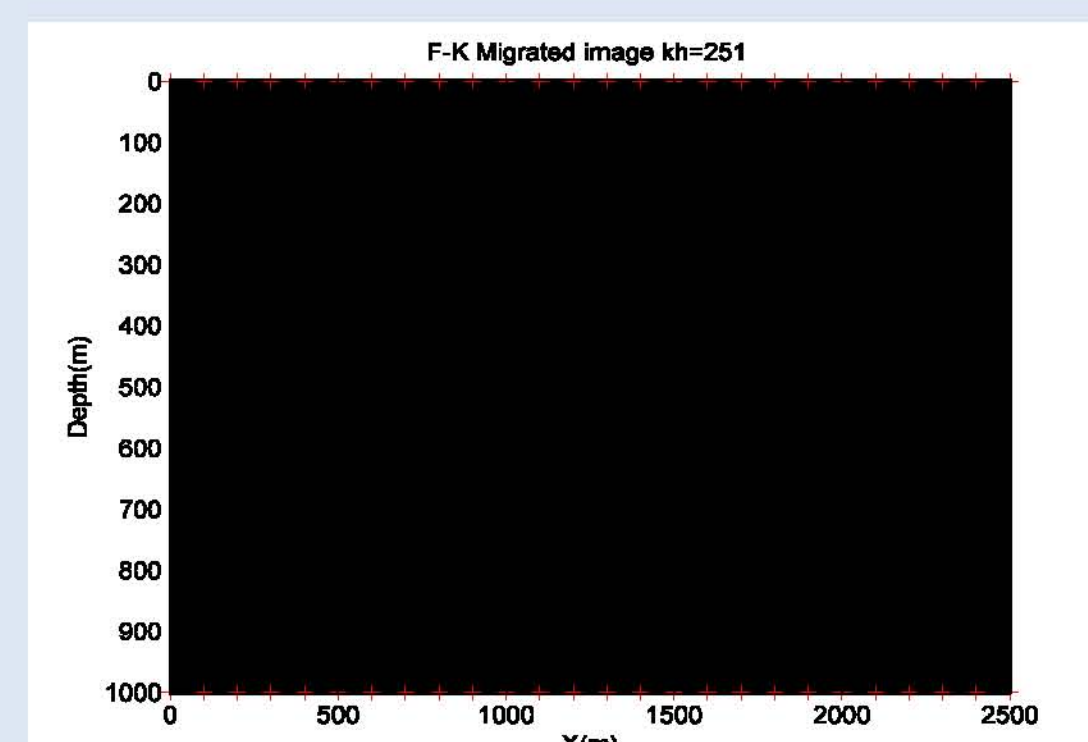


Figure 2: 2-Layer Horizontal Model, Migrated Image

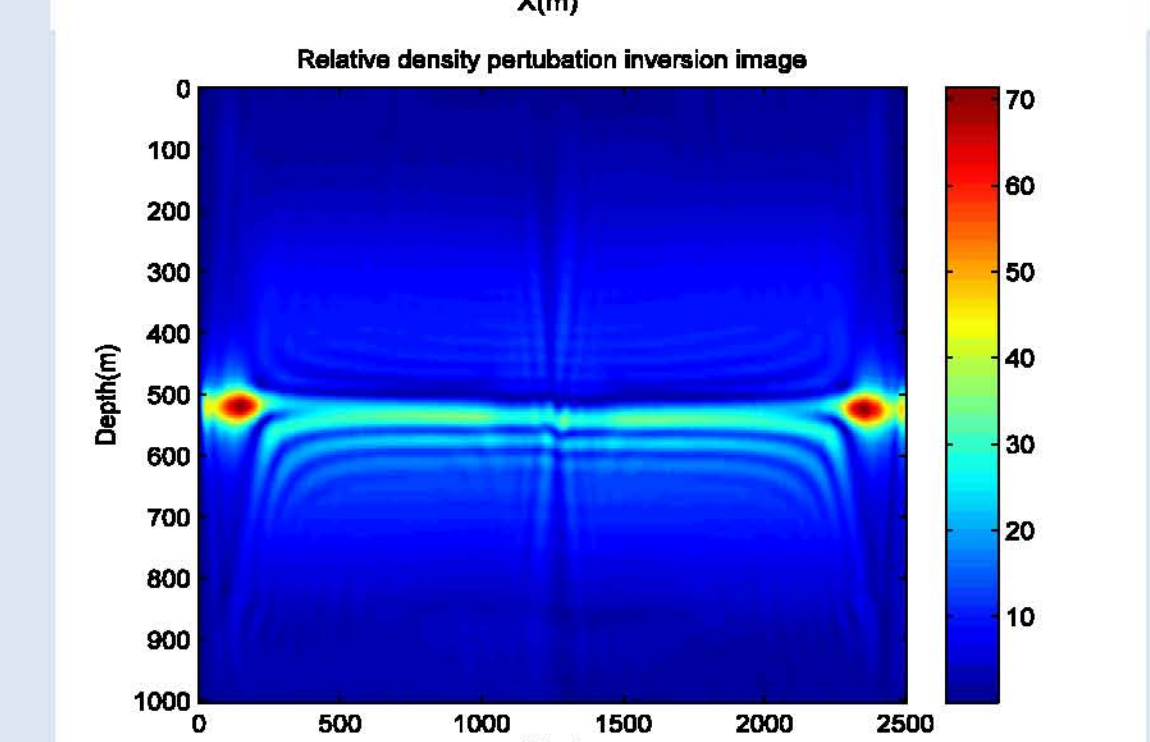
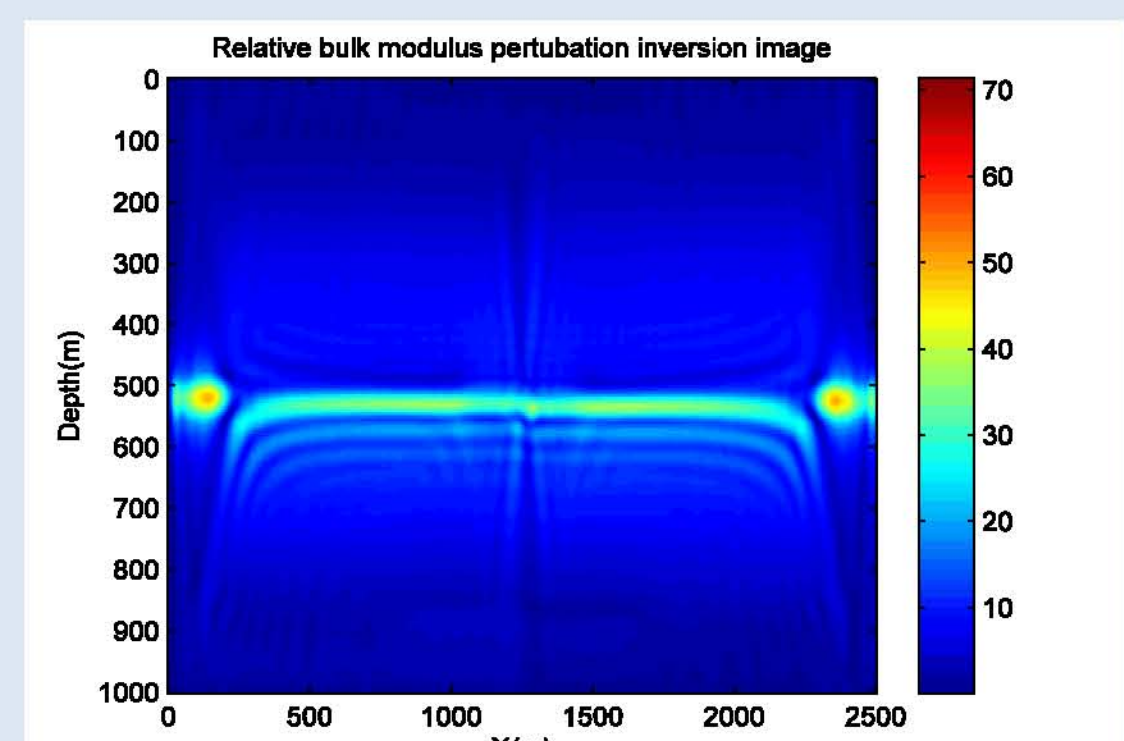


Figure 3a: Perturbation in bulk modulus for 2 layers

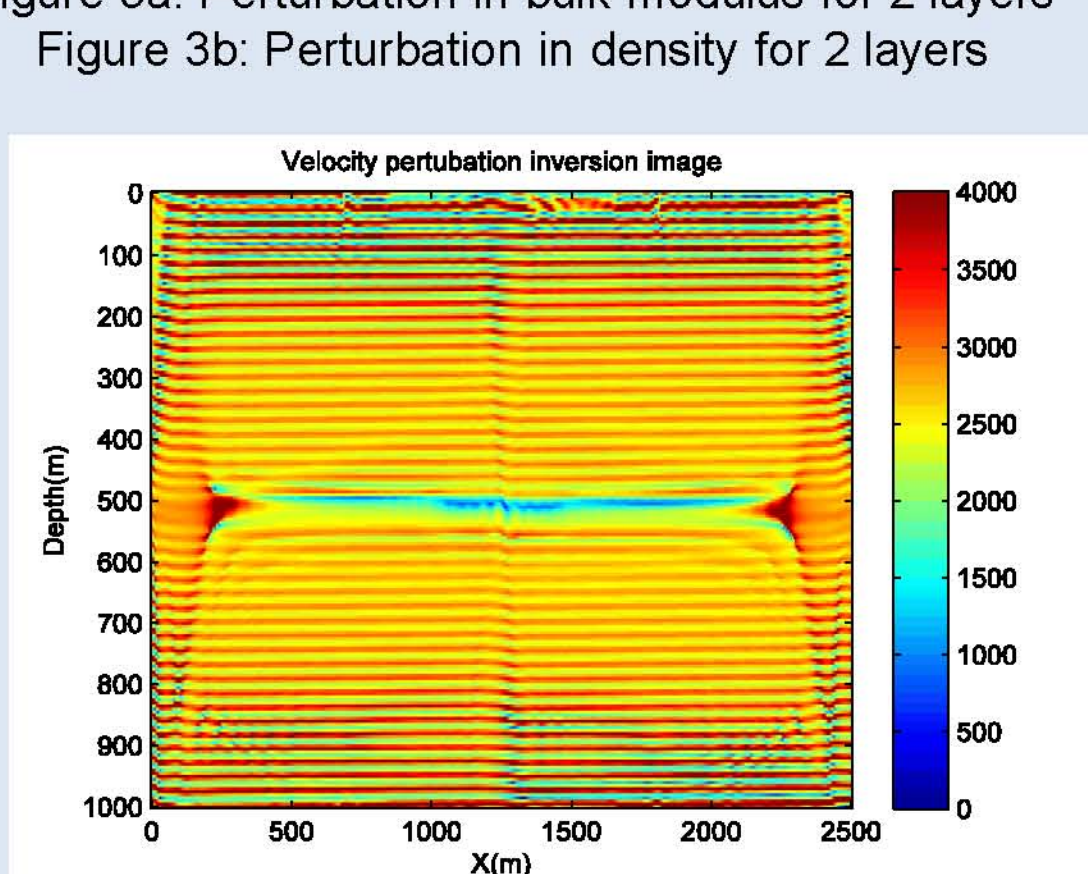


Figure 3b: Perturbation in density for 2 layers

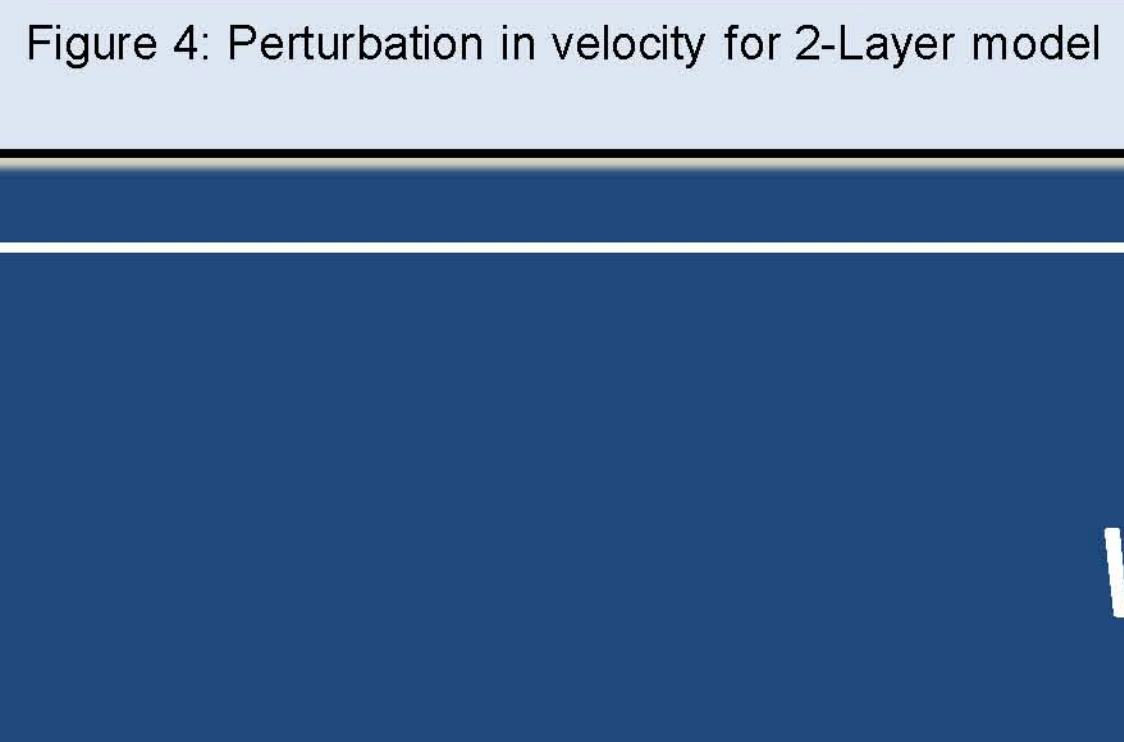


Figure 4: Perturbation in velocity for 2-Layer model

Four layer horizontal model

The four layer model demonstrates a slightly more complex environment. Figure 5 shows the migrated image and figures 7a, 7b the inversion images showing the perturbation in K and ρ . As can be seen, the magnitude of the perturbation at each interface increases with depth. This is expected as the magnitude of the difference in model velocity from the background velocity increases with depth. The resulting velocity perturbation image in figure 8 has the correct location of the velocity perturbations. The amplitude of the perturbations is less than expected and will require some investigation.

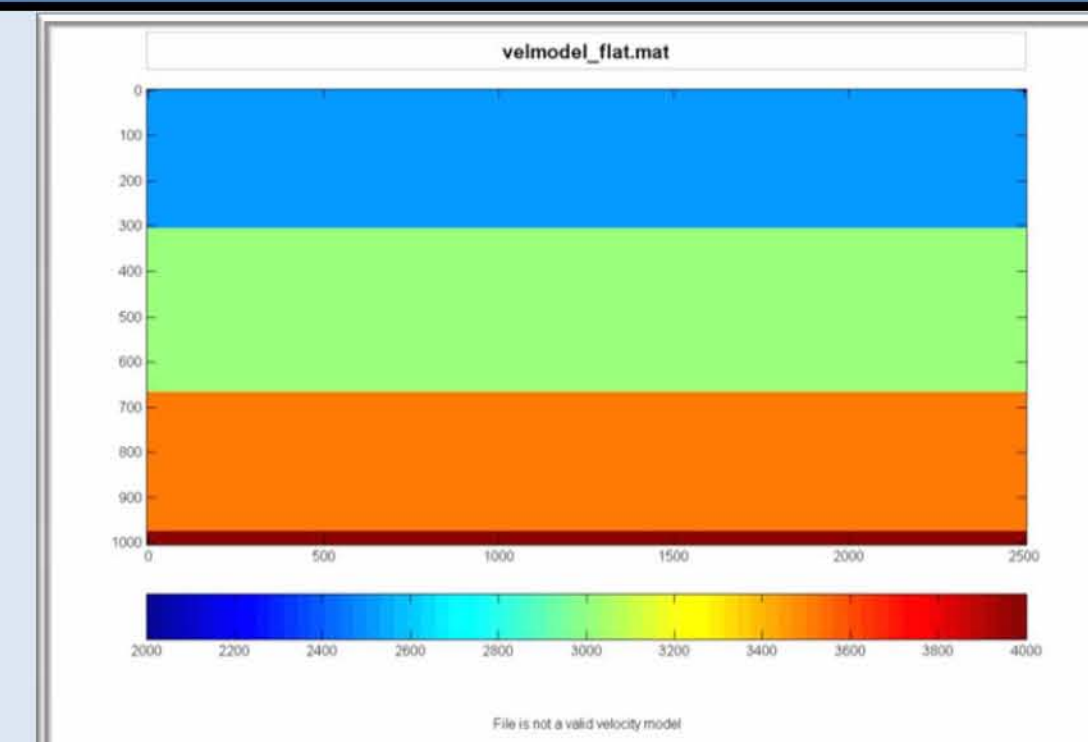


Figure 5: Four Layer Horizontal Velocity Model

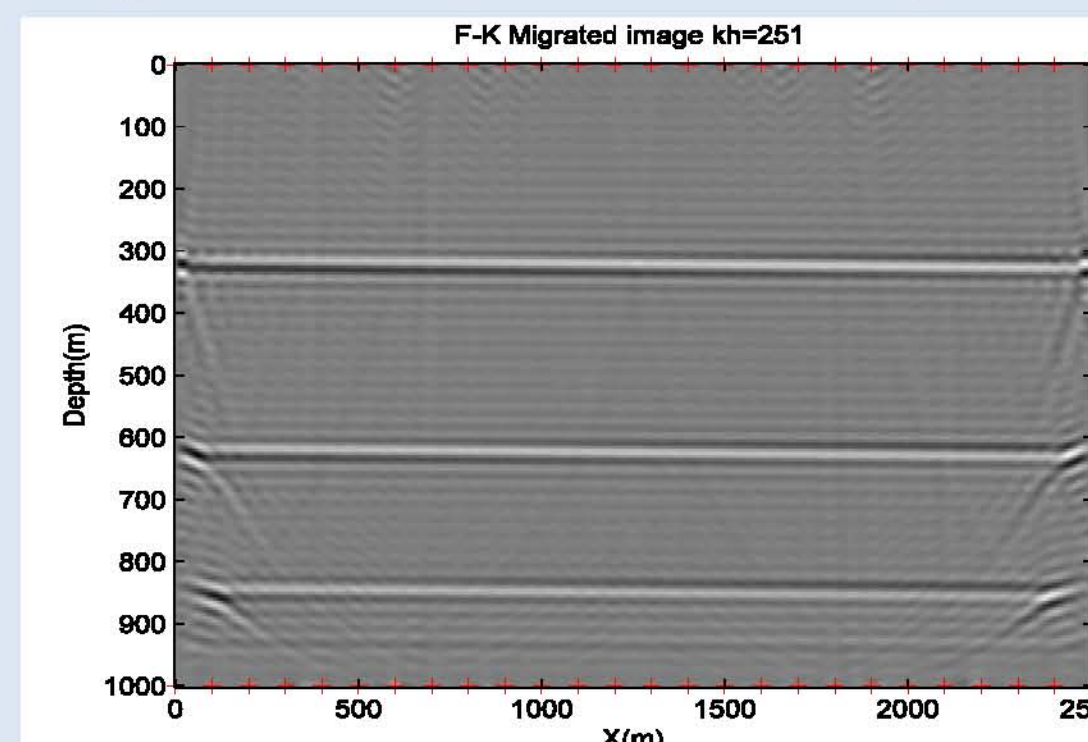


Figure 6: Four Layer Horizontal, Migrated Image

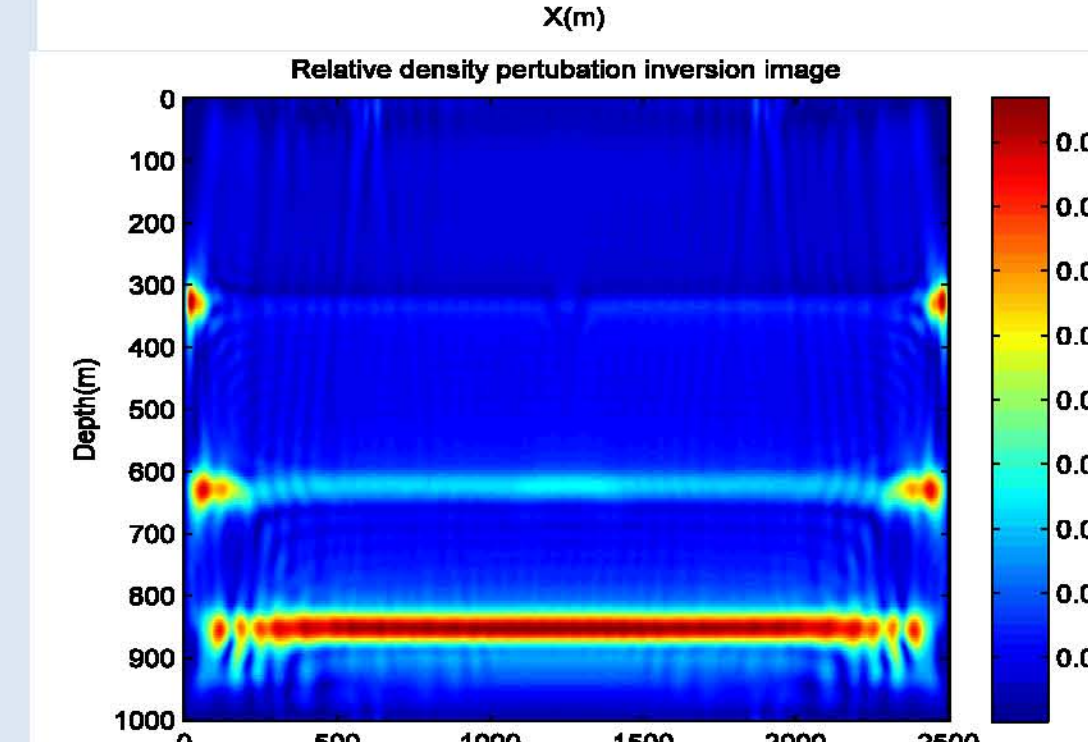
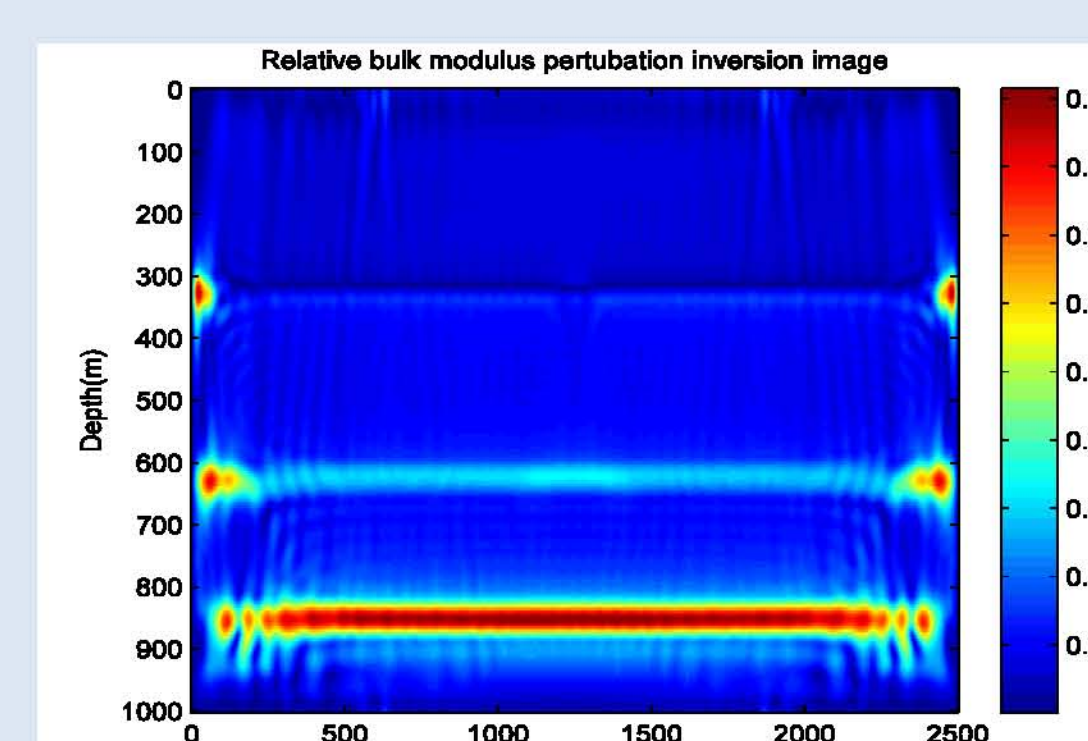


Figure 7a: Perturbation in bulk modulus for 4 layers

Figure 7b: Perturbation in density for 4 layers

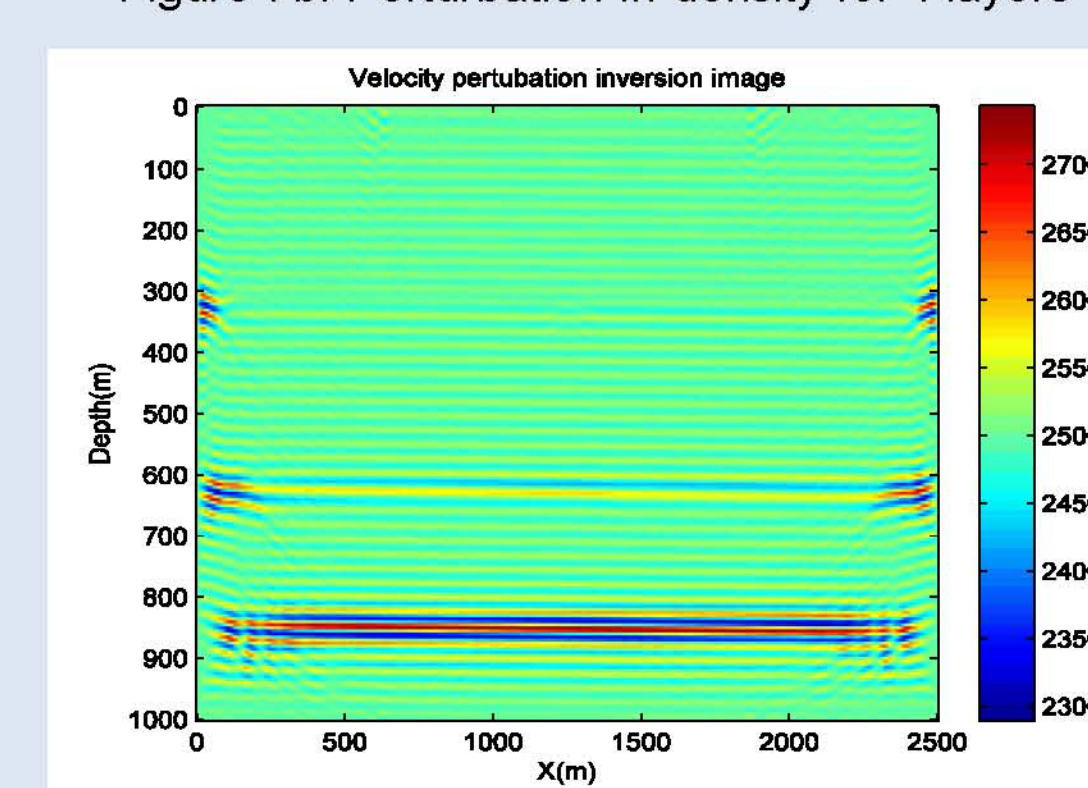


Figure 8: Perturbation in velocity for 4-Layer model

Low velocity model

The shallow, low velocity model was created to see if the inversion properly placed the deep reflectors when encountering a low velocity layer. In this case we have a biconvex lens. Figure 10 shows the effects of a low velocity medium and the distortions in the apparent positions of deeper layer. The perturbation images in figures 11a and 11b display some features caused by the coarseness of the original model. This includes overlapping diffraction patterns and a 'beading' effect along the perturbation boundaries.

What is correct is the lack of multiple reflections which are clearly visible in the migration image, but missing from the perturbation images. This is because we are only computing first order scattering terms so multiples or higher order scattering contributions are missing. Again there is a small but noticeable difference in perturbation amplitude scales. An effect of unequal sampling in kz and kh domains.

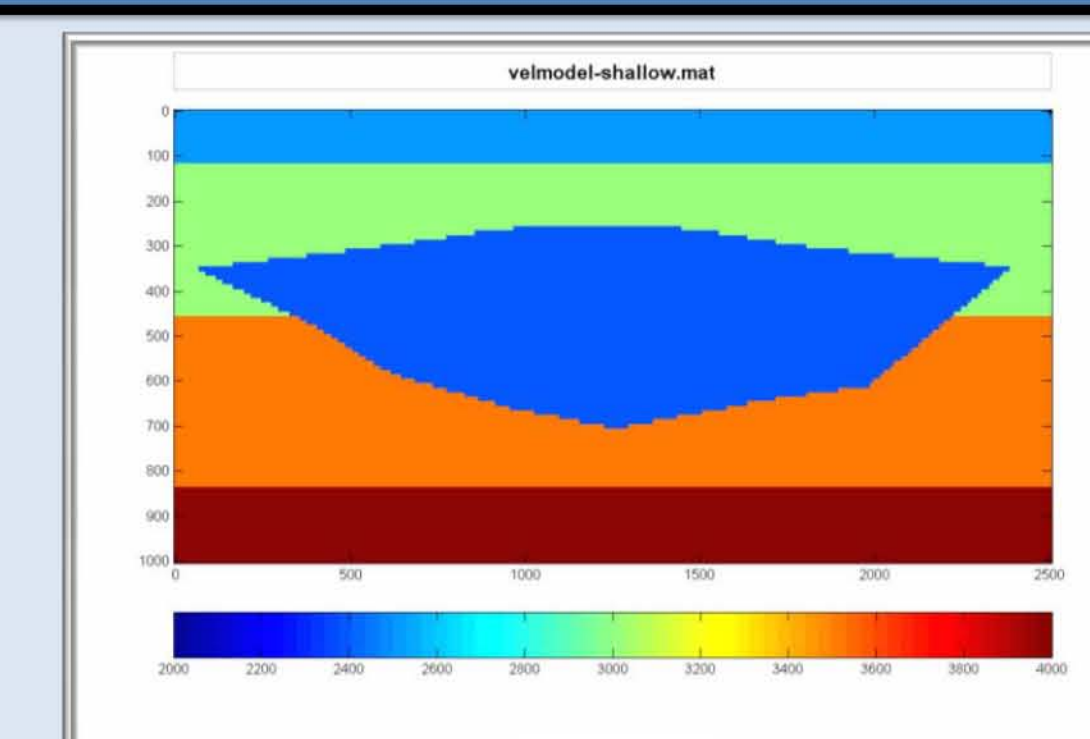


Figure 9: Shallow Lens Velocity Model

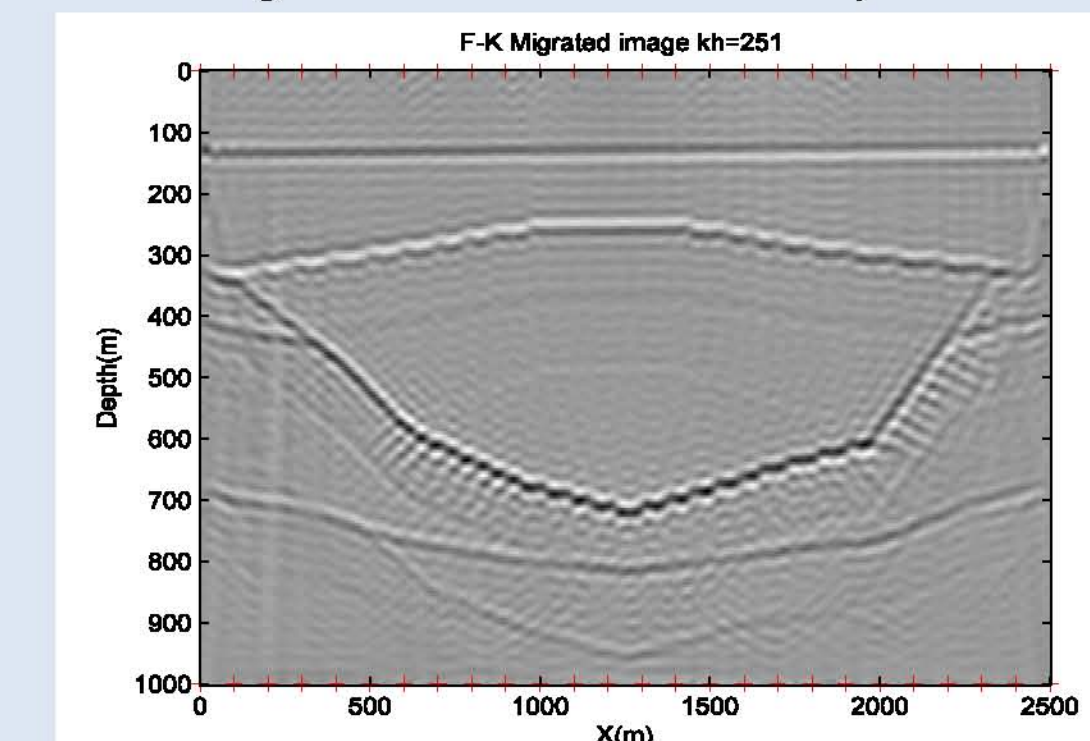


Figure 10: Shallow Lens Model, Migrated Image

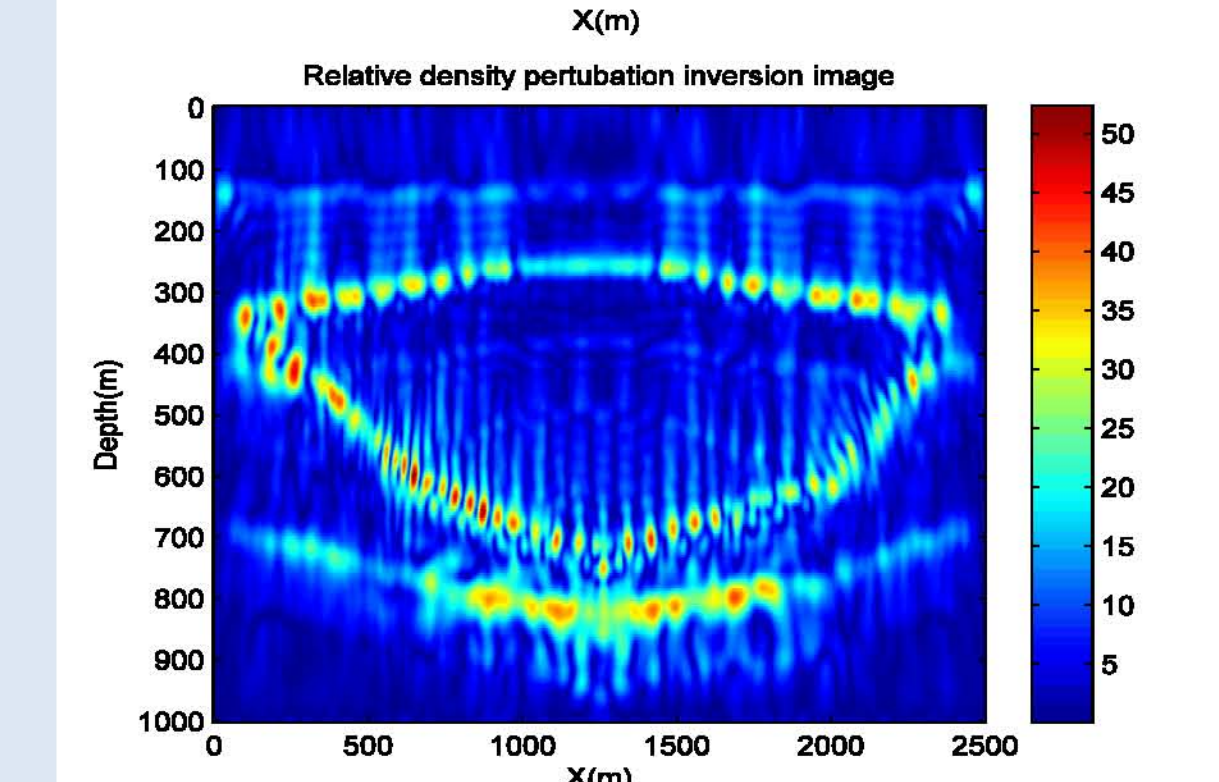
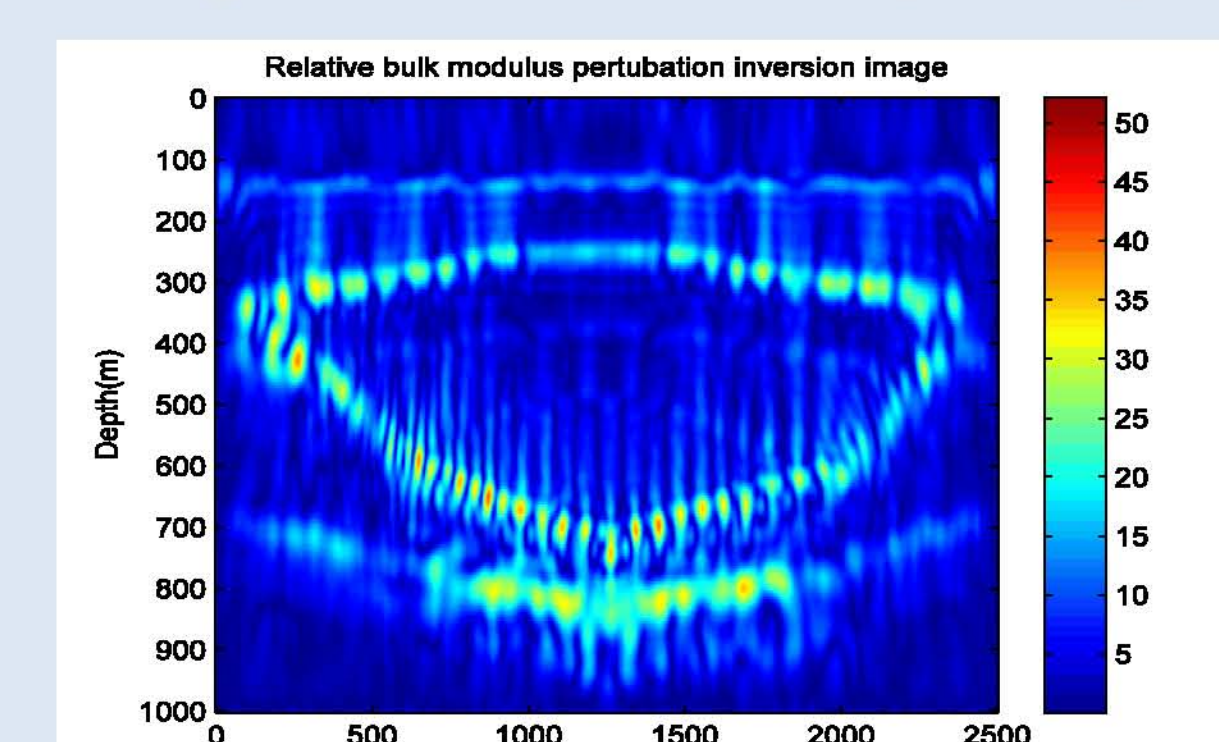


Figure 11a: Perturbation in bulk modulus for shallow lens

Figure 11b: Perturbation in density for shallow lens

Anticline velocity model

The Anticline velocity model shown in Figure 12 also has a low velocity center but has a concave upper surface and a convex lower surface which should create significant distortion. Like the low velocity model there are distortions and effects caused by diffractions from the sharp corners of the model. Again the random noise is minimized and the multiple reflections are missing from the results in figures 14a and 14b.

What is different in this run is the very noticeable difference in the perturbation intensities between 14a and 14b. This is due to the use of a greater number of offsets, kh, then in other model runs. An artificial resolution issue was introduced when the ratio of kz/kh was not maintained which caused an emphasis in the resolution of shallower layers relative to the deeper layers (see the report for more details).

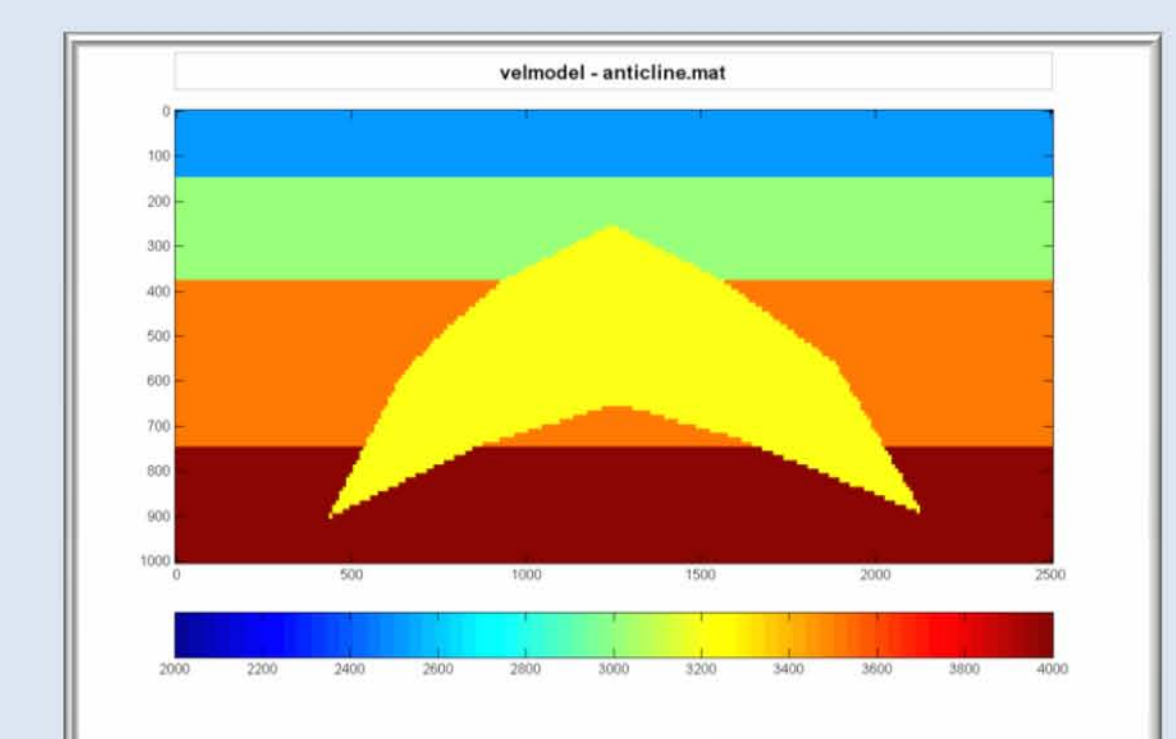


Figure 12: Anticline Velocity Model

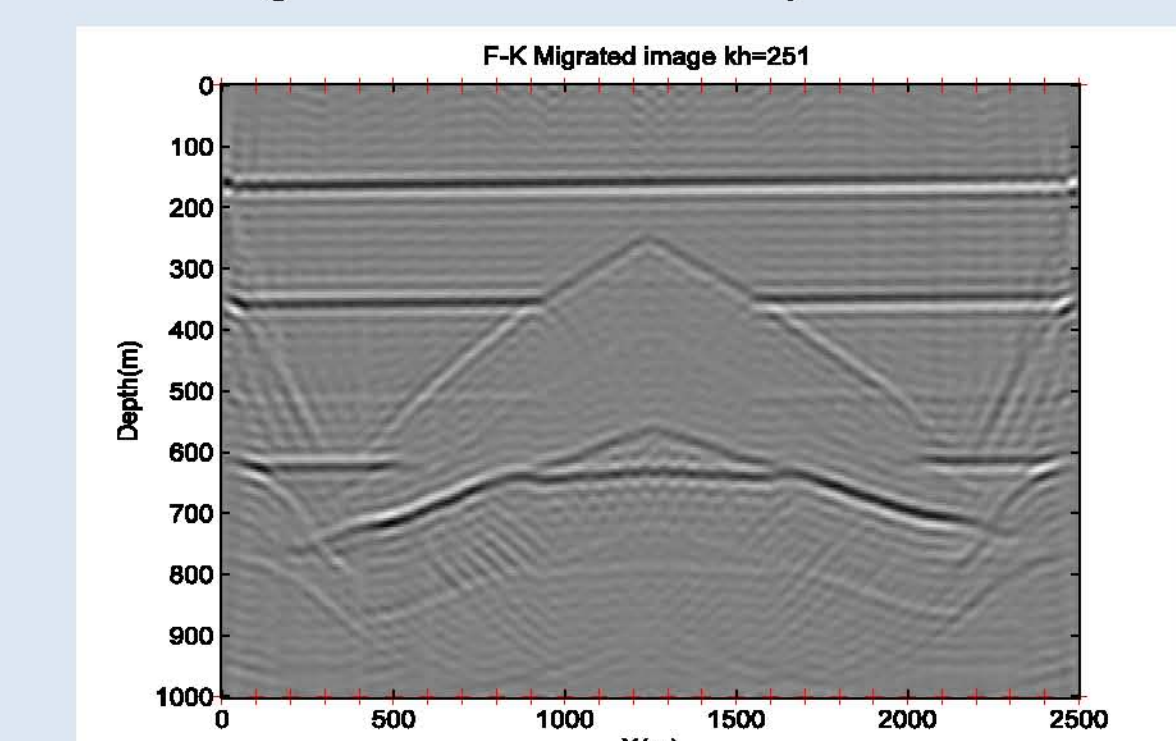


Figure 13: Anticline Model, Migrated Image

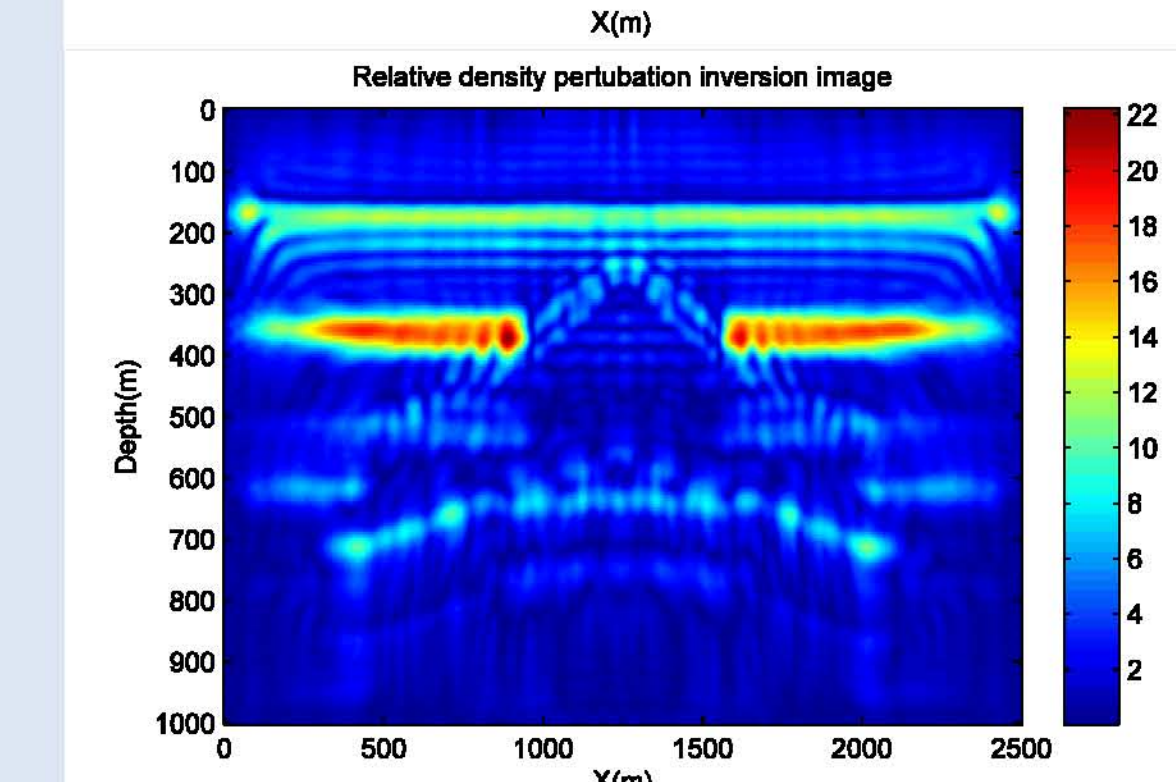
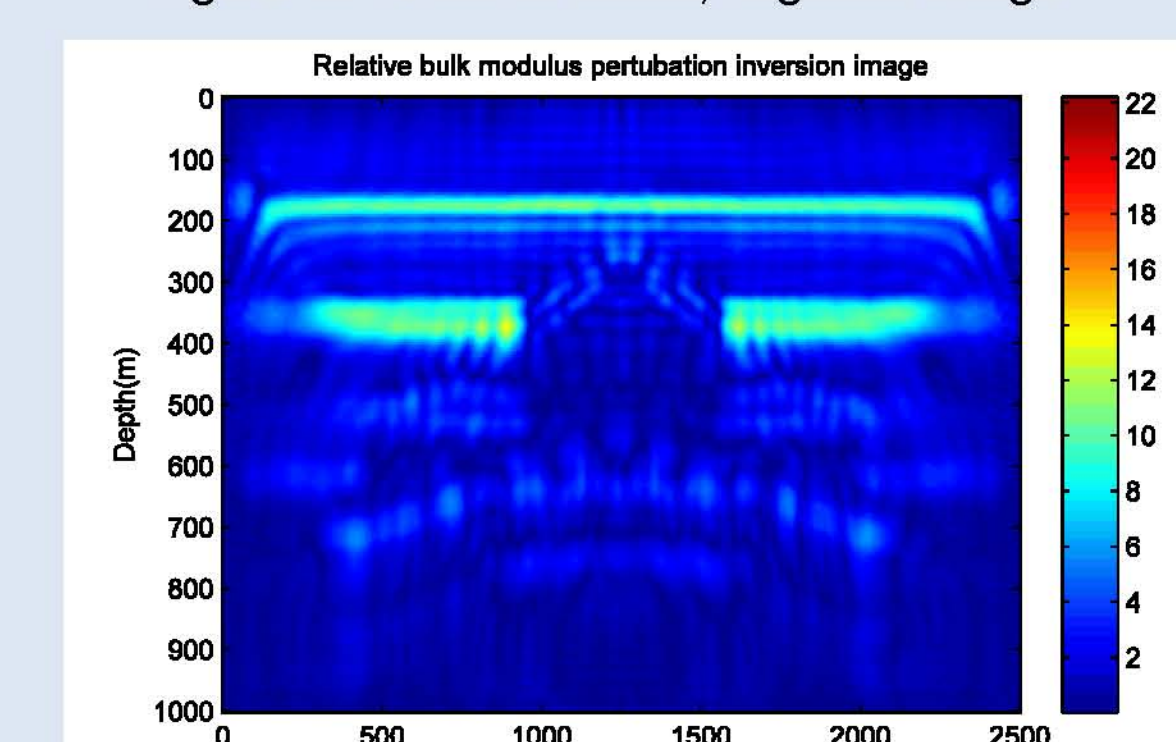


Figure 14a: Perturbation in bulk modulus for anticline

Figure 14b: Perturbation in density for anticline